Biochimica et Biophysica Acta 1830 (2013) 3643–3649

Contents lists available at SciVerse ScienceDirect

Biochimica et Biophysica Acta

journal homepage: www.elsevier.com/locate/bbagen

Synthesis of 3-O-methylgallic acid a powerful antioxidant by electrochemical conversion of syringic acid

Olfa Dridi Gargouri, Boutheina Gargouri, Souhel Kallel Trabelsi, Mohamed Bouaziz *, Ridha Abdelhédi

Laboratoire d'Electrochimie et Environnement, Ecole Nationale d'Ingénieur de Sfax, BP 1173, 3038 Sfax, Université de Sfax, Tunisia

ARTICLE INFO

Article history:
Received 11 October 2012
Received in revised form 2 February 2013
Accepted 11 February 2013
Available online 20 February 2013

Keywords:
Syringic acid
3-O-methylgallic acid
Anodic oxidation
Cyclic voltammetry
Antioxidant activity

ABSTRACT

Background: A kinetic study of the electrochemical oxidation of syringic acid (3,5-dimethoxy-4-hydroxybenzoic acid) by cyclic voltammetry at treated gold disk was combined with results of electrolyses at Ta/PbO_2 anode in order to convert it into potentially high-added-value product.
Methods: The electrochemical oxidation of syringic acid was carried out in order to convert this compound to 3-O-methylgallic acid. This latter was identified by mass spectrophotometry using LC-MS/MS apparatus. The 3-O-methylgallic acid synthesis was controlled by cyclic volammetry, Ortho-diphenolicdeterminations and DPPH radical-scavenging activity.
Results: The proposed mechanism is based on the hypothesis of a bielectronic discharge of syringic acid molecule under free and adsorbed form involving two intermediate cation mesomers. Hydrolysis of the more stable of this last one leads to the formation of the 3,4-dihydroxy-5-methoxybenzoic acid (3-O-methylgallic acid) as a major product. The latter aromatic compound was synthesized by anodic oxidation of syringic acid at PbO2 electrode. The cyclic voltammogram of the electrolysis bath of syringic acid shows that the anodic peak potential of 3-O-methylgallic acid was lower (E_{pa} = 128 mV) than that of SA (E_{pa} = 320 mV). And the strongest antiradical activity was detected when the 3-O-methylgallic acid concentration was higher".
Conclusion: The electrochemical oxidation using PbO_2 anode is a rapid, simple and efficient method tool for a conversion of SA into 3-O-methylgallic acid, a potent antioxidant derivative
General Significance: The electrochemical process consists in a simple transformation of the syringic acid into 3-O-methylgallic acid having a better antioxidant capacity. This result has been justified by cyclic voltametry which shows that anodic peak of 3-O-methylgallic acid is reversible. Furthermore, its potential is lower than that of the irreversible anodic peak of syringic acid to 3-O-methylgallic acid.

1. Introduction

Phenolic compounds are a complex group of substances that have attracted considerable attention due to their roles in providing flavor and color characteristics of food and in human health [1]. Higher concentration of these compounds is found in olive and mainly in olive mill wastewater. Phenolic compounds may vary in structure due to difference in number and position of the hydroxyl groups on the aromatic ring. As a group, these naturally occurring compounds have been found to be strong antioxidants against free radicals and other reactive oxygen species (ROS) which constitute the major cause of many chronic human diseases such as cancer and cardiovascular diseases [2,3].

Compounds which are antioxidants by virtue of their ability to act as reductants in solution tend to be easily oxidized at inert electrodes. In this context, cyclic voltammetry has been applied to characterize a range of antioxidants, including phenolic acids and flavonoids [4–8], ascorbic acid [9], and synthetic antioxidants [10,11]. It has been reported [12,13] that the chemical structure of the side chain, as well as the number and position of free hydroxy and methoxy groups attached to the aromatic ring played key roles in the antioxidant activity of the phenolic acids. Moreover, the decrease of the oxidation potential of these compounds leads generally to an increase of their antioxidant activity [14]. The electrochemical oxidation mechanism of the phenolic compounds has been well discussed [15–18].

It has been well recognized that this last one undergoes a first monoelectronic transfer leading to the formation of phenoxy radicals. This first step should be ascribed to the antioxidant activity of these compounds. Depending on their structure and the magnitude of the anodic potential, the phenoxy radicals can lead to the formation of polymers and/or hydroquinonic (*p*-hydroquinones and catechol derivatives) and benzoquinonic (*p* and *o*-benzoquinone derivatives) structures [17–20]. The reversible anodic oxidation of *p* and *o*-hydroquinone structures occurs at lower potentials than those of the starting monophenols [17,21]. In the contrary, the anodic oxidation of their oxidized forms (*p* and *o*-benzoquinonic structures) is irreversible and more difficult than that of the starting monophenols [14,16,17]. According to our previous work, Table 1 shows the relative values of anodic oxidation potentials

* Corresponding author. Tel.: +216 98667581.
E-mail address: mohamed.bouaziz@fsg.rnu.tn (M. Bouaziz).

0304-4165/$ – see front matter © 2013 Elsevier B.V. All rights reserved.
http://dx.doi.org/10.1016/j.bbagen.2013.02.012

Table 1
Potential values of anodic peaks of phenol, hydroquinone and *p*-benzoquinone. Electrode: pre-treated Pt disk (r = 1 mm), Q = 4 mC, T = 25 °C [22].

Compounds	Potential anodic peak (V/SHE)
Phenol	1.11
Hydroquinone	0.63
p-Benzoquinone	1.23

of phenol and its oxidation products namely the *p*-hydroquinone and *p*-benzoquinone [22].

Syringic acid (SA) (3,5-dimethoxy-4 hydroxybenzoic acid) has been investigated by cyclic voltammetry at a glassy carbon electrode [14]. In this context, Alaexandra et al. [14] have observed that syringic acid has a very poor radical scavenging activity and higher oxidation potential in comparison with protocatechuic acid and caffeic acid [14,23,24].

The present study concerns the electrochemical behavior of SA in aqueous solutions. We were interested at first in the kinetic study of the first stages of the oxidation mechanism of SA by cyclic voltammetry at electrodes of Au/Au oxides. These oxidation steps are those that precede the opening of the aromatic ring. Gold is often regarded as the ideal solid electrode for fundamental electrochemical investigation as it is difficult at this metal to completely oxidize aromatic compounds. The electrocatalytic properties of Au/Au oxide electrode were characterized by the charge Q corresponding to the electrochemical formation of the gold oxides. Besides, we showed in a previous work that the charge Q allows control of electrocatalytic properties of the Au/Au oxide electrode [16,17,25]. In the second part of this work, we will use a Ta/PbO_2 anode in view to convert SA into a product having an important biological activity. It should be noted that at low anodic potential, PbO_2 behaves like gold vis-à-vis the aromatic compound oxidation [26]. On the other hand, the antiradical ability of SA and its oxidation products has been assessed by measuring the ease of their reaction with the stable free radical diphenylpicrylhydrazyl (DPPH$^{\bullet}$) leading to its reduced form (DPPH-H). Good free radical scavengers react fast leaving small amounts of unreduced DPPH, which indicates the presence of an effective antioxidant [23].

2. Experimental

2.1. Reagents and chemicals

Sodium molybdate dehydrate and organic solvents were purchased from Merck (Darmstadt, Germany). Syringic acid (SA), 2,2-diphenyl-1-picrylhydrazyl (DPPH), and all other chemicals were purchased from Sigma–Aldrich (St. Louis, MO). All reagents and chemicals used were of analytical grade.

2.2. Apparatus

A potentiostat type PJT Tacussel was used for electrochemical measurements and the data was recorded using a GSTP4 Tacussel X-Y recorder. The charge Q corresponding to the electrochemical formation of the gold oxides was measured using an IG6-N Tacussel integrator. In this investigation, all the potentials refer to $Hg/Hg_2SO_4/K_2SO_4$ electrode ($E = +0.61$ V/SHE).

2.3. Treatment of the gold electrodes

The working electrode was a polycrystalline gold disk of ca. 0.0314 cm^2 exposed area. This electrode was mechanically polished with a fine alumina powder ($\varphi = 0.3$ μm) and washed with ultrapure water before transfer to the cell. The electrode was then subjected to potential cycling conditions, in sulfuric acid (0.5 mol L^{-1}), between −610 and +1190 mV vs. a saturated mercurous sulfate at a scan rate of 300 V min^{-1} for a period depending on the desired oxide layer thickness. The initially bright gold electrode became red brown. The electrochemical response of the treated electrode is presented in Fig. 1 (curve 1). The cyclic voltammogram was characterized by a large anodic peak at +760 mV corresponding to the Au oxide formation and a cathodic peak at +500 mV relative to the Au oxide reduction. The gold oxide electrode was characterized by the charge Q corresponding to the electrochemical formation of the gold oxides [25]. Q was considered as the main characteristic of the electro-active surface.

2.4. Electrolysis

Galvanostatic electrolysis of SA in aqueous solutions was carried out in an isothermal reactor with two compartments. The electrolytic solution treated (V = 150 cm^3) initially contained SA (2 mmol L^{-1}) in H_2SO_4 (pH = 1.8). The Ta/PbO_2 anode was placed in front of the cathode; the opposite face of plate relative to the cathode was masked with a protective film (transparent polyethylene tape, Scotch TM 480. 3 M). The total surface area of the working electrode was 4 cm^2. Experimental details for the preparation of Ta/PbO_2 were described in our previous work [17]. The cathode was a bar of graphite ($\varphi = 1$ cm, L = 6 cm) placed in a porous ceramic cylinder (Norton, Refractaire RA 84) containing 1 mol L^{-1} sulfuric acid solution. The acid solution of SA was electrolyzed at 30 °C, with magnetic stirring and under a constant anodic current density of 15 mA cm^{-2}.

2.5. LC–MS/MS analysis

Liquid chromatography–mass spectrometry (LC–MS) of the SA after 240 min of electrolysis was performed on an Agilent 1100 series LC-MSD. The compounds were separated with a Zorbax 300 A° Extend-C-18 column (2.1 × 150 mm, particle size 5 μm, Agilent Technology, INC, Wilmingtom, DE, USA). The mobile phase was a mixture of two solvents formic acid (1%) in water (A) and methanol:acetonitrile:formic acid (89.5:9.5:1, v/v/v) (B). Analysis conditions were as described before [27]. The percentage by volume of (B) varies linearly with time as follows: from 10 to 30% for the first 10 min, then from 30 to 40% up to 25 min after isocratic during 5 min, from 40 to 50% up to 40 min and from 50 to 100% up to 50 min, after that back to 10% up to 55 min and finally isocratic up to 65 min. The column outlet was coupled with an Agilent MSD ion trap XCT mass spectrometer (Santa Clara, CA, USA) equipped with an ESI ion source.

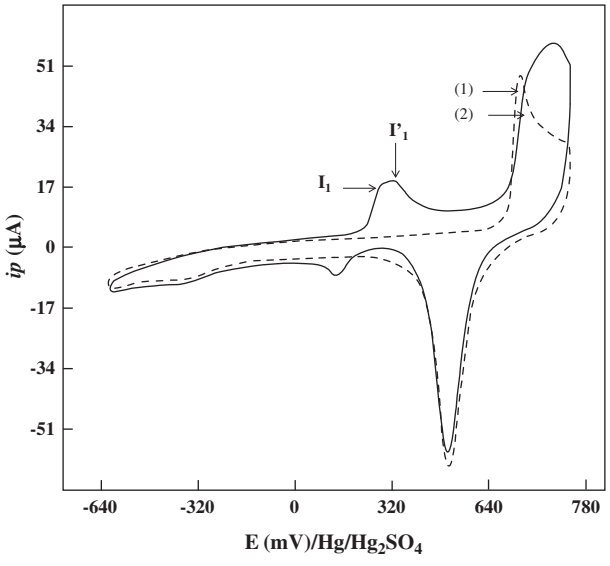

Fig. 1. Cyclic voltammograms recorded on a disk of gold ($\varphi = 1$ mm). Q = 0.22 mC; v = 50 mV s^{-1}; T = 20 °C; H_2SO_4 = 0.5 mol L^{-1}; SA concentration: (1) 0; (2) 0.6 mmol L^{-1}.

2.6. Ortho-diphenolic determinations

Ortho-diphenolic content was determined following the previously modified method described by Cert et al. [28]. This method is based on the formation of yellow complex between ortho-diphenols and molybdate ions. Briefly, 2 mL of sample was added to 0.5 mL of sodium molybdate dihydrate solution (0.5 g L^{-1}, in a mixture ethanol/water, 1/1, v/v). The mixture was shaken, and after 15 min at room temperature, the absorbance was measured at 370 nm. Standards of gallic acid were prepared similarly.

2.7. Determination of DPPH radical-scavenging activity

The DPPH (2,2-diphenyl-1-picrylhydrazyl) radical scavenging effect was evaluated following the procedure described in a previous study [29]. Aliquots (50 μL) of various concentrations (5, 10, 15, 20 and 25 μg/mL) of the test extracts in methanol were added to 5 mL of methanolic solution containing DPPH radicals (6×10^{-6} mol L^{-1}). After 30 min incubation period at room temperature and in the dark, the absorbance was read in opposition to the control at 517 nm. The Inhibition (IC_{50}) of free radical DPPH (IC_{50}%) was calculated in percentage: $IC_{50}\% = [(A_{blank} - A_{sample})/A_{blank}]\times 100$, where A_{blank} is the absorbance of the control reaction (containing all reagents except the test extract), and A_{sample} is the absorbance of the test extract. The concentration of the test extract providing 50% inhibition (IC_{50}, expressed in μg mL^{-1}) was calculated from the graph plotted with inhibition percentage against the extract concentration. The synthetic antioxidant reagent butylated hydroxytoluene (BHT) was used as positive control and all tests were carried out in triplicate.

3. Results and discussion

3.1. Voltammetric study

The SA oxidation was first studied by cyclic voltammetry at treated gold electrode. A typical voltammogram for the oxidation of 0.6 mmol L^{-1} SA solution in sulfuric acid (0.5 mol L^{-1}) at a scan rate of 50 mV s^{-1} is shown in Fig. 1 (curve 2). During the first forward positive scan, SA exhibits two anodic peaks I_1 and I'_1 at $E_{pa} = 270$ and $E'_{pa} = 320$ mV respectively. The successive cyclic voltammograms of 4 mmol L^{-1} SA solution at the same electrode are presented in Fig. 2. From the second cycle, the voltammograms exhibit a reversible peak I_2 at 128 mV which is ascribed to the oxidation of the majority SA oxidation product.

Moreover the relative importance of the two peaks I_1 and I'_1 depends on the SA concentration, the potential scan rate and the Q value characterizing the state of the treated gold surface.

3.1.1. Influence of SA concentration

Fig. 3 regroups some of the first cyclic voltammograms recorded at treated gold electrode characterized by a Q value of 0.22 mC in SA aqueous solution at concentrations ranging from 0.1 to 4 mmol L^{-1}. For SA concentration less than 0.2 mmol L^{-1}, only the peak I_1 is observed. With increasing SA concentration above 0.2 mmol L^{-1} the peak I'_1 appears. When the SA concentration increases the current intensities $ip(I_1)$ (Fig. 4 curve 1) and $ip(I'_1)$ (Fig. 4 curve 2) of these peaks increase then tend towards around 16 and 12 μA respectively.

3.1.2. Influence of the charge (Q)

Some cyclic voltammograms are recorded for 0.6 mmol L^{-1} SA aqueous solution at treated gold electrodes characterized by Q values in the range 0.15–0.33 mC.Fig. 5 shows that currents $ip(I_1)$ and $ip(I'_1)$ increase linearly with Q value.

3.1.3. Influence of the potential scan rate

From voltammograms presented in Fig. 6, we have shown that the current $ip(I_1)$ varies linearly with the square root of the potential scan rate v (Fig. 7a). The slope of the straight line representing $ip(I_1)$ as a function of the square root of the potential scan rate gives the diffusion coefficient D of SA by application of Eq. (A.1).

$$ip(I_1) = 2.69 \cdot 10^5 \; S \; n^{3/2} D_{red}{}^{1/2} v^{1/2} C \qquad (A.1)$$

where n is the number of exchanged electrons; S is the electrode surface area (cm^2); D is diffusion coefficient (cm^2 s^{-1}); v is the scan rate (V s^{-1}); and C is the SA concentration (mol cm^{-3}).

The diffusion coefficient of SA calculated for $n = 2$, is $4.46\cdot10^{-6}$ cm^2 s^{-1} at 25 °C. Although to our knowledge this diffusion coefficient has not previously been estimated, its value found in this work is situated in the range of compounds having a similar structure which undergo a bielectronic discharge [16].

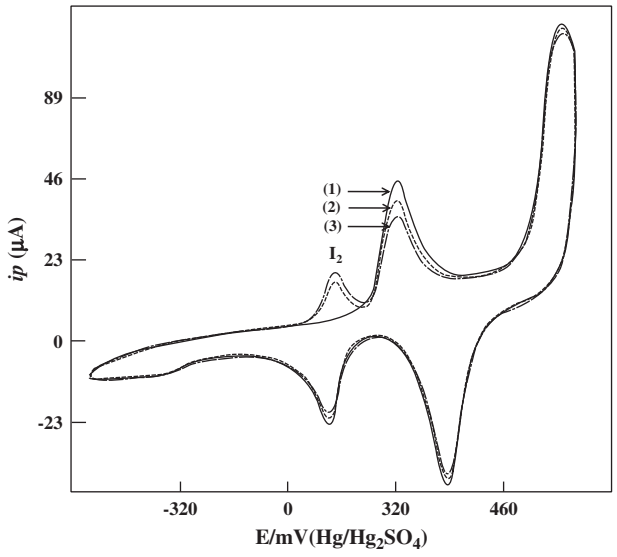

Fig. 2. Successive cyclic voltammograms of SA (4 mmol L^{-1}) at gold disk in sulfuric acid aqueous solution at potential scan rate of 50 mV s^{-1}; Q = 0.22 mC; H_2SO_4 = 0.5 mol L^{-1}; SA concentration 4 mmol L^{-1}; (1): 1th, (2): 2th, (3): 3th cycle.

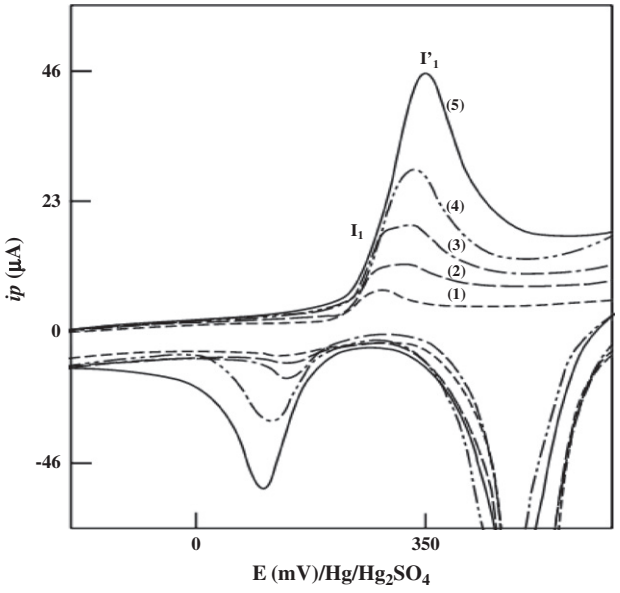

Fig. 3. Cyclic voltammograms of SA at a disk of gold (φ = 1 mm). Q = 0.22 mC; v = 50 mV s^{-1}; T = 20 °C; H_2SO_4 = 0.5 mol L^{-1}; SA concentration: (1) 0.1; (2) 0.4; (3) 0.8; (4) 2; (5) 4 mmol L^{-1}.

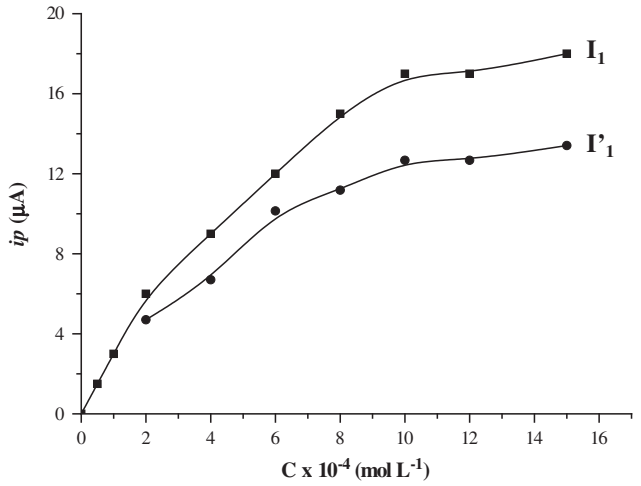

Fig. 4. Variation of the current of the peaks I_1 and I'_1 as function of SA concentration. Q = 0.22 mC; v = 50 mV s^{-1}; T = 20°C; H_2SO_4 = 0.5 mol L^{-1}.

On the other hand, the voltammograms shown in Fig. 6 show that when the potential scan rate increases, $ip(I'_1)$ rises more than $ip(I_1)$.

The results presented above may be interpreted by assuming that the electrochemical oxidation of SA molecules takes place on the treated gold electrode by electron transfer for both free and adsorbed forms. The free form corresponds to the first peak I_1 while the strongly adsorbed form, which is consequently stabilized, is oxidized at a more anodic potential and corresponds to the "post-peak" I'_1.

The adsorption aspect of the peak I'_1 is confirmed according to the procedure already undertaken in previous studies in the case of the oxidation of phenol at platinum [21]. The treated gold electrode is immersed into SA aqueous solution then rinsed in ultrapure water and immediately subjected to potential cycling in 0.5 mol L^{-1} sulfuric acid aqueous solution. The voltammogram shows only a single anodic peak which appears towards 320 mV. This peak which results from the oxidation of the adsorbed SA coincides with the peak I'_1. Its current intensity varies linearly with potential scan rate v (Fig. 7(b)) according to Eq. (A.2).

$$ip\left(I'_1\right)_{ads} = \frac{n^2F^2}{4RT} S v \Gamma \qquad (A.2)$$

where Γ is the superficial concentration (mol cm^{-2}) of adsorbed SA.

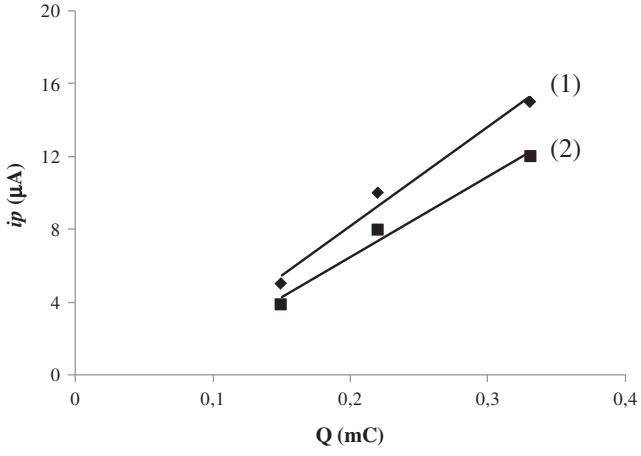

Fig. 5. Variation of the current of the peaks I_1 and I'_1 as a function of the charge Q. v = 50 mV s^{-1}, v = 50 mV s^{-1}, SA concentration: 0.6 mmol L^{-1}. (1) $ip(I_1)$; (2) $ip(I'_1)$.

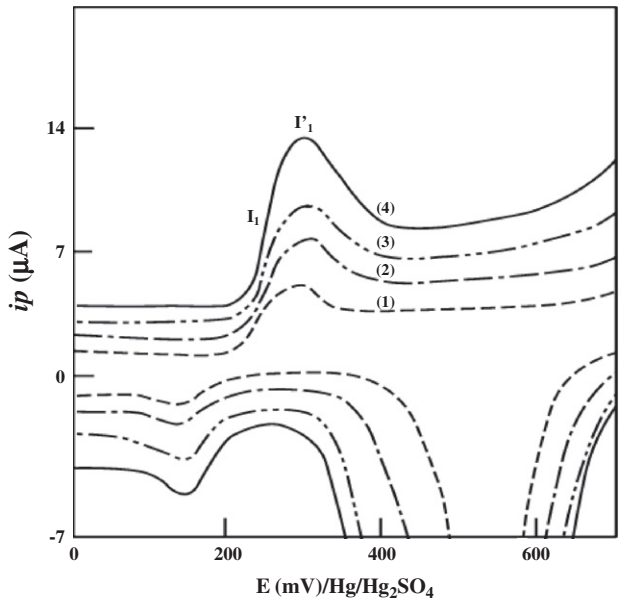

Fig. 6. Cyclic voltammograms of SA at a disk of gold (φ = 1 mm).Q = 0.22 mC; T = 20 °C; H_2SO_4 = 0.5 mol L^{-1}; SA concentration: 0.6 mmol L^{-1}; potential scan rate: (1) 10; (2) 25; (3) 50; (4) 70 mV s^{-1}.

3.2. Electrochemical oxidation of SA at PbO_2 anode

The electrochemical oxidation of 2 mmol L^{-1} SA aqueous solution at PbO_2 anode under 15 mA cm^{-2} was followed by cyclic voltammetry at treated gold electrode. Fig. 8(a) shows cyclic voltammograms at different electrolysis time. The initial voltammogram for untreated solution (t = 0 min) showed only the oxidation peak I'_1 of SA at E'_{pa} = 320 mV/(Hg/Hg_2SO_4).

The following voltammograms, exhibit the reversible anodic peak I_2 which has been previously observed during the cyclic voltammetric study (Fig. 2). The current of this peak reaches its maximum at about 5 µA after 240 min of oxidation, then decreases. However, the current of the peak I'_1 decays until zero after 360 min (Fig. 8(b)).

To elucidate the structures of SA aromatic products obtained after 240 min electrolysis, a sample was analyzed by liquid chromatography with electrospray mass spectrometry in the negative mode. The structure assignment of these products was based on UV absorbance spectra with a systematic search for molecular ions using extracted ion mass chromatograms and comparing the MS/MS spectra with those in the literature [30].

Compound **1** was identified to SA retained at 16.8 min (Fig. 9). The spectrum MS^1 exhibits a molecular ion at m/z 197 $[M–H]^-$. The MS^2 spectrum obtained by fragmentation of this ion presents the following m/z values: 182, 153, 138 and 121. The fragmentation of the pseudo molecular ion $[M–H]^-$ at m/z 197 yields a fragment at m/z 182 by the loss of 15 mass units. The ion m/z 153 by the loss (−44) of a carboxylic acid group, providing an anion of [M–H–COO]−. The ions at m/z 138 and 121 are fragments of ion m/z 153 by the loss of methyl radical (−15) and water molecule. This profile is compatible with syringic acid that has been described by Gruz et al. [30]. The LC–MS analysis of compound **2** (Fig. 10) produced a negative ion of m/z 183, corresponding to the $[M–H]^-$ precursor ion. Subsequent product ion scan (MS^2) of this precursor ion produced a fragmentation pattern dominated by an ion at m/z 168 $[M–CH_3–H]^-$. The loss (−44) of a carboxylic acid group, providing an anion (m/z 139) of $[M–H–COO]^-$. In addition, we detected an ion at m/z 124 explained by the loss of methyl radical (−15) from methoxylated derivatives of compound **2** leading to a very stable anion radical structure of $[M–H–COO\text{-}CH_3]^-$. In accordance with our findings, Gruz et al. [30], noted analogous collision-induced fragmentation of deprotonated (poly-)methoxylated phenolic acid and flavonoids,

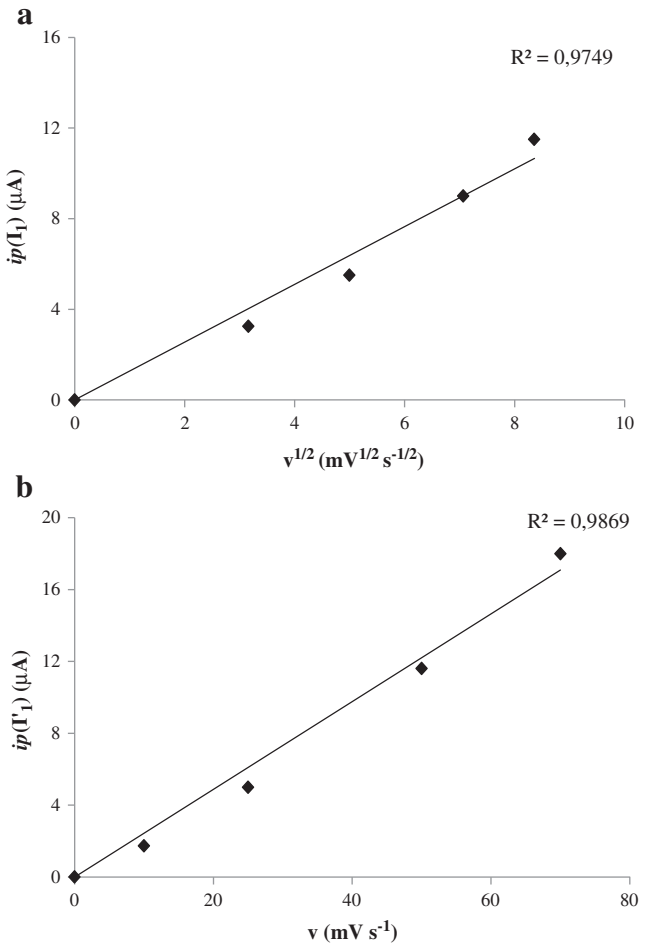

Fig. 7. Variation of the current of the peaks I_1 and I'_1 as function of potential scan rate, SA concentration: 0.6 mmol L^{-1}; Q = 0.22 mC; T = 20 °C; H_2SO_4: 0.5 mol L^{-1}; *v*: 10; 25; 50 and 70 mV s^{-1}.

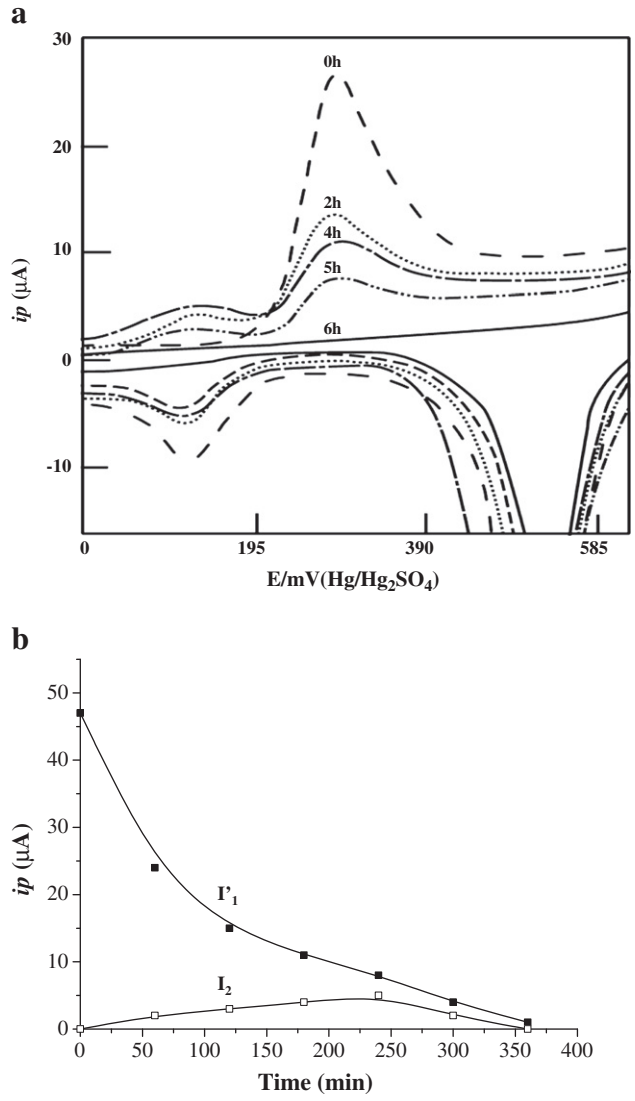

Fig. 8. (a) Cyclic voltammograms of 2 mmol L^{-1} SA at gold disk in sulfuric acid aqueous solution at potential scan rate of 50 mV s^{-1} as a function time electrolysis of SA at PbO_2. (b) Variation of current $ip(I_2)$ and $ip(I'_1)$ during anodic oxidation of SA, j_{app} = 15 mA cm^2, pH = 1.8, T = 30 °C.

respectively, distinguished by specific losses of methyl radicals from their respective $[M–H]^-$ anions. This suggested that **2** might be a 3-O-methylgallic acid. The mass spectrum of compound **3** (retention time 4.1 min) exhibited a base peak at m/z 167 $[M–H]^-$ in negative ion mode and strong peaks at m/z 152 $[M–H\text{-}CH_3]^-$. This observation can be a diagnosis of synergic acid quinone derivatives. The combined results of the MS and UV spectra suggest that compound **3** could be 2,6-dimethoxybenzoquinone. The latter was confirmed by chromatography with authentic standards as 2,6 dimethoxybenzoquinone.

The principal aromatic compounds, identified by LC/MS, are 3-O-methylgallic acid and 2,6-dimethoxybenzoquinone. These results are in good agreement with the proposed SA oxidation mechanism.

3.3. Antioxidant activity

The DPPH radical-scavenging activities of SA solution treated by anodic oxidation at PbO_2 were investigated during electrolysis (Fig. 11). The low IC_{50} values designated potent radical-scavenging effects, as low concentrations were adequate to inhibit the DPPH radicals [13,31].

All samples exhibited antioxidant activity, which showed correlation between orthodiphenol content and DPPH radical-scavenging activity over all anodic oxidation of SA.

The SA which presents a single hydroxyl group has IC_{50} = 90 mg L^{-1}, confers a limited amount of antioxidant activity. On the other hand, the lower IC_{50} values (16 mg L^{-1}), which indicated higher antioxidant potential, were observed for the samples harvested at 240 min of electrolyses. This is probably due to the significant radical inhibition caused by a high concentration of *o*-diphenol such as 3-O-methylgallic acid. The antioxidant activity and the level of the orthodiphenol content in the SA solution treated suggest that the radical scavenging effect in the solution can be attributed to hydroxylated phenolic compounds, in particular, the number of hydroxyl substituents in the aromatic ring and the nature

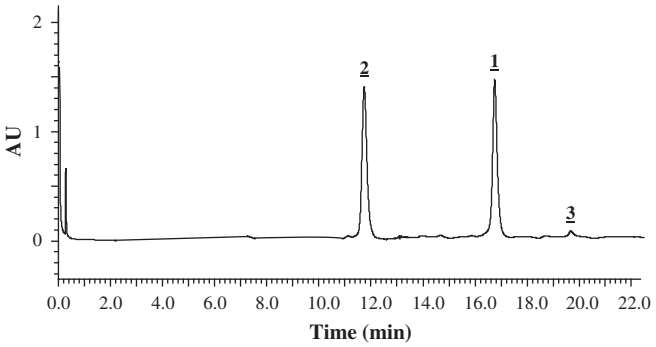

Fig. 9. HPLC chromatograms at 280 nm after 240 min SA anodic oxidation at PbO_2. **1**: syringic acid; **2**: 3-O-methylgallic acid; **3**: 2,6 dimethoxybenzoquinone.

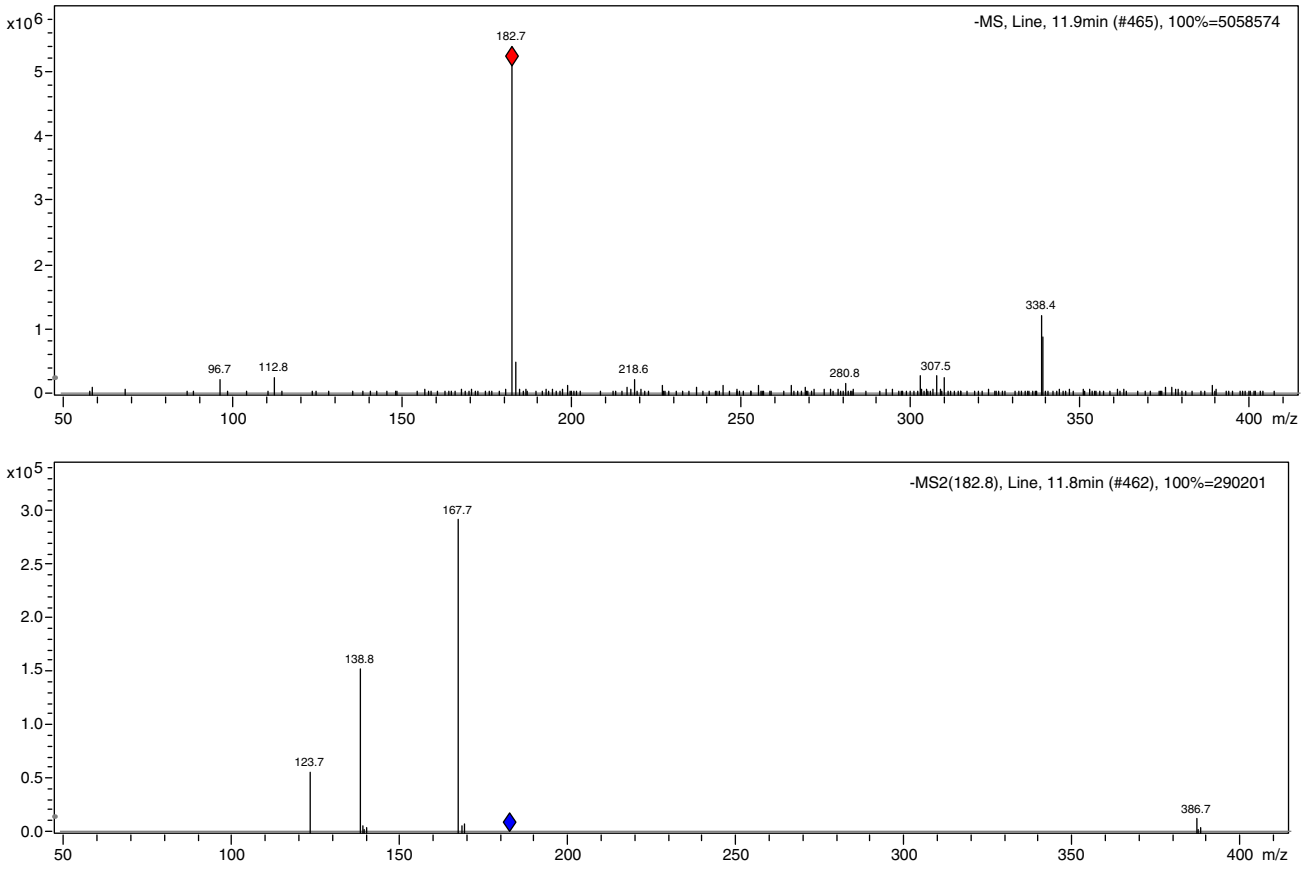

Fig. 10. LC–MS/MS spectrum ($MS^1$and MS^2) of SA after 240 min SA anodic oxidation at PbO_2, j_{app} = 15 mA cm^{-2}; pH = 1.8; T = 30 °C.

of the substituents at the para or ortho position [13]. These compounds react with free radicals formed during autoxidation and generate a new radical that is stabilized by the resonance effect of the aromatic nucleus [24]. So 3-O-methylgallic acid exhibited antioxidant activity at a level similar to that of BHT (IC_{50} = 17 mg L^{-1}).

Cyclic voltammetry has been applied to characterize the reducing ability of natural phenolics [6,32] and good correlations have been observed between redox potentials and antioxidant properties [33,34]. In accordance with the global mechanism proposed for SA oxidation, the hydroxyl groups are oxidized via two electron transfer leading to the generation of a correspondent quinone after liberation of $2H^+$. These results indicated that the higher number of hydroxyl substituents on the aromatic ring, correspond to the lower electrochemical potential.

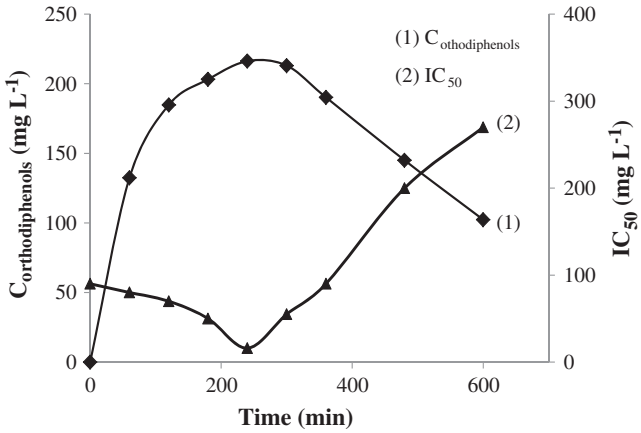

Fig. 11. Free radical scavenging activity and ortho-diphenol tests during anodic oxidation of SA at PbO_2. Other conditions as in Fig. 8.

Thus, SA (monophenol) have a higher potential (E_{pa} = 320 mV) than 3-O-methylgallic acid (E_{pa} = 128 mV).

3.4. Oxidation mechanism of the SA

The preceding results allow to schematize the oxidation mechanism of SA in Fig. 12. SA molecules undergo a first electron transfer under free and adsorb forms leading to the formation of phenoxy radicals for which the electronic charge distribution can be represented by three mesomeric forms A, B and C. By considering the electronic effects of methoxy and carboxy groups, the radical B would be the most probable. The formation of 3-O-methylgallic acid (B_3) could be explained assuming that the radical B undergoes a second electron transfer leading to the carbocation B_1 which gives simultaneously the 3-methoxy-4,5-dioxobenzoic acid (B_2) and a methanol molecule by hydrolysis. During the reverse scan, the 3-methoxy-4,5-dioxobenzoic acid (B_2) is reduced to 3-O-methylgallic acid (B_3) at the potential of the reversible peak I_2. Moreover, the proportions of SA oxidation product formed via the intermediary of the less probable radical C would be insignificant. The oxidation of this last one leads to the formation of 2,6-dimethoxy-p-hydroquinone (C_2) which is oxidized to 2,6-dimethoxy-p-benzoquinone (C_2).

4. Conclusion

From these studies, it was concluded that electrochemical oxidation using PbO_2 anode is a rapid, simple and efficient method tool for conversion of SA into a potent antioxidant derivative. Using LC–MS, it was possible to determine the structure of 3-O-methylgallic acid and the other phenolics produced during electrochemical treatment.

The measured oxidation potential was closely related to the structures. The phenolic structure influences also antioxidant activity. The ortho-diphenol compound has lower anodic peak potential and higher

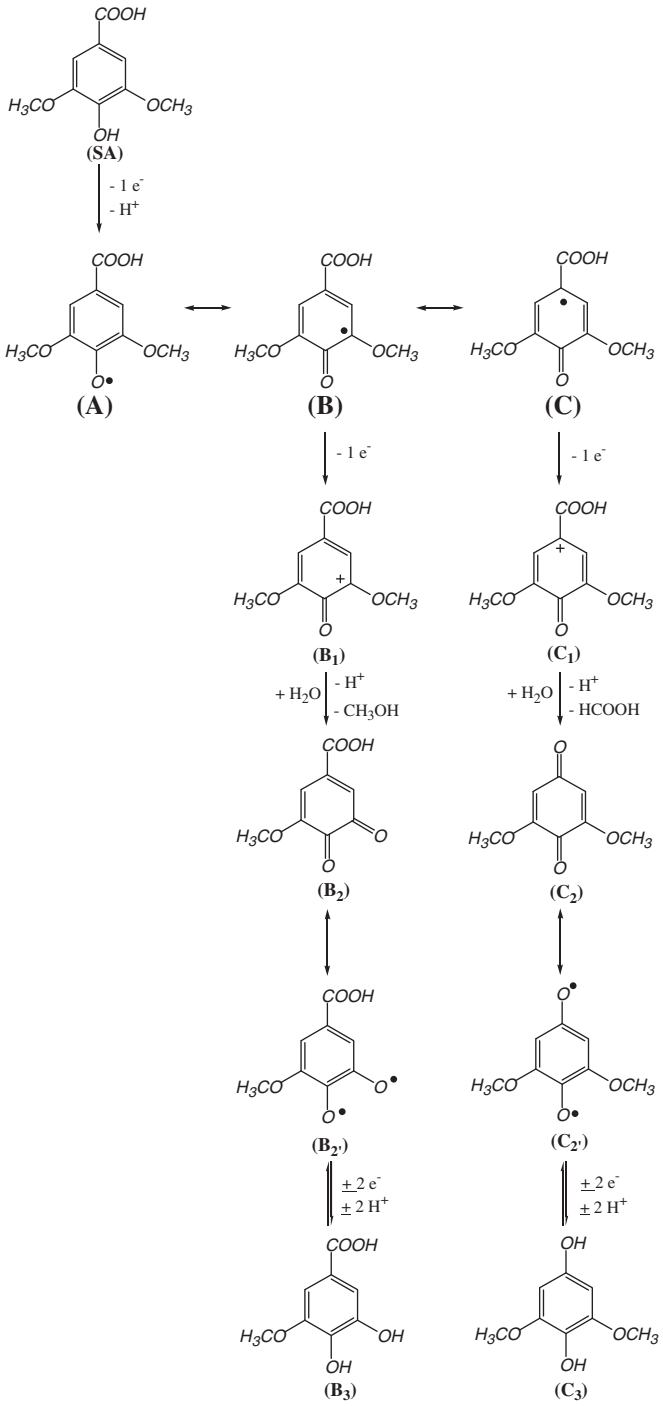

Fig. 12. Oxidation pathways of SA in aqueous sulfuric acid medium at treated gold.

antioxidant ability than monosubstituted phenol (SA), although OH groups have stronger effects than OCH_3 ones. In addition, the change in the phenolic contents reflected their antioxidant properties. These compounds could make significant contributions to the health benefits associated with the consumption of various food ingredients.

References

[1] M. Bouaziz, S. Lassoued, Z. Bouallagui, S. Smaoui, A. Gargoubi, A. Dhouib, S. Sayadi, Synthesis and recovery of high bioactive phenolics from table-olive brine process wastewater, Bioorg. Med. Chem. 16 (2008) 9238–9246.

[2] M.F. Andreasen, P.A. Kroon, G. Williamson, M.T. Garcia-Conesa, Esterase activity able to hydrolyze dietary antioxidant hydroxycinnamates is distributed along the intestine of mammals, J. Agric. Food Chem. 49 (2001) 5679–5684.

[3] L. Yu, S. Haley, J. Perret, M. Harris, J. Wilson, M. Qian, Free radical scavenging properties of wheat extracts, J. Agric. Food Chem. 50 (2002) 1619–1624.

[4] H.P. Hendrickson, A.D. Kaufman, C.E. Lunte, Electrochemistry of catechol-containing flavonoids, J. Pharm. Biomed. Anal. 12 (1994) 325–334.

[5] M. Born, P.A. Carrupt, R. Zini, F. Bree, J.P. Tillement, K. Hostettmann, B. Testa, Electrochemical behavior and antioxidant activity of some natural polyphenols, Helv. Chim. Acta. 79 (1996) 1147–1158.

[6] P. Hapiot, A. Neudeck, J. Pinson, H. Fulcrand, P. Neta, C. Rolando, Oxidation of caffeic acid and related hydroxycinnamic acids, J. Electroanal. Chem. 405 (1996) 169–176.

[7] L.V. Jorgensen, L.H. Skibsted, Flavonoid deactivation of ferrylmyoglobin in relation to ease of oxidation as determined by cyclic voltammetry, Free Radic. Res. 28 (1998) 335–351.

[8] G.K. Budnikov, G.K. Ziyatdinova, Antioxidants as analytes in analytical chemistry, J. Anal. Chem. 60 (7) (2005) 600–613.

[9] M.H. Pournaghi-Azar, R. Ojani, A selective catalytic voltammetric determination of vitamin C in pharmaceutical preparations and complex matrices of fresh fruit juices, Talanta 44 (1997) 297–303.

[10] E. Diego, L. Agui, A. Gonzales-Cortes, P. Yanez-Sedeno, J.M. Pingarron, J.M. Kauffman, Critical comparison of paraffin carbon paste and graphite-poly(tetrafluorethylene) composite electrodes concerning the electroanalytical behavior of various antioxidants of different hydrophobicity, Electroanalysis 10 (1998) 33–38.

[11] Y. Ni, L. Wang, S. Kokot, Voltammetric determination of butylated hydroxyanisole, butylated hydroxytoluene, propyl gallate and tert-butylhydroquinone by use of chemometric approaches, Anal. Chim. Acta 412 (2000) 185–193.

[12] F. Natella, M. Nardini, M. Di Felice, C. Scaccini, Benzoic and cinnamic acid derivatives as antioxidants: structure–activity relation, J. Agric. Food Chem. 47 (1999) 1453–1459.

[13] M. Bouaziz, R.J. Grayer, M.S.J. Simmonds, M. Damak, S. Sayadi, Identification and antioxidant potential of flavonoids and low molecular weight phenols in olive cultivar Chemlali growing in Tunisia, J. Agric. Food Chem. 53 (2005) 236–241.

[14] A. Simié, D. Manojlović, D. Segan, M. Todorović, Electrochemical behavior and antioxidant and prooxidant activity of natural phenolics, Molecules 12 (2007) 2327–2340.

[15] N. Belhadj Tahar, A. Savall, Electropolymerization of phenol on a vitreous carbon electrode in alkaline aqueous solution at different temperatures, Electrochim. Acta 55 (2009) 465–469.

[16] S.K. Trabelsi, N. Belhadj Tahar, B. Trabelsi, R. Abdelhedi, Electrochemical oxidation of ferrulic acid in aqueous solutions at gold oxide and lead dioxide electrodes, J. Appl. Electrochem. 35 (2005) 967–973.

[17] S.K. Trabelsi, N. Belhadj Tahar, R. Abdelhedi, Electrochemical behavior of caffeic acid, Electrochim. Acta 49 (2004) 1647–1654.

[18] M. Gattrell, D.W. Kirk, A study of the oxidation of phenol at platinum and peroxidized platinum surfaces, J. Electrochem. Soc. 140 (1993) 1534–1540.

[19] L. Papouchado, R.W. Sandford, G. Petrie, R.N. Adams, Anodic oxidation of phenolic compounds part 2. Stepwise electron transfers and coupled hydroxylations, J. Electroanal. Chem. 65 (1975) 275–284.

[20] N. Belhadj Tahar, A. Savall, Mechanistic aspects of phenol electrochemical degradation by oxidation on Ta/PbO_2 anode, J. Electrochem. Soc. 10 (1998) 3427–3433.

[21] R.W. Sousa, C. da Rocha, C.L. Cardoso, S.D.H. Silva, B.M.V. Zanoni, Determination of the relative contribution of phenolic antioxidants in orange juce by voltammetric methods, J. Food Compos. Anal. 17 (2004) 619–633.

[22] Y. Samet, R. Mefteh, R. Abdelhedi, A. Savall, Improvement of the electrocatalytic activity of platinum in oxidation of aromatic compounds, C. R. Chimie 11 (2008) 1254–1261.

[23] V. Bonded, B.W. Williams, C. Berset, Kinetics and mechanisms of antioxidant activity using DPPH free radical methods, Lebensm.-Wiss. Technol. 30 (1997) 609–615.

[24] M.E. Cuvelier, H. Richard, C. Berset, Comparison of the antioxidative activity of some acid phenols: structure–activity relation ship, Biosci. Biotechnol. Biochem. 56 (1992) 324–325.

[25] R. Abdelhedi, M.L. Bouguerra, Passivation d'Electrodes de Platine et d'Or lors de l'Oxydation Electrochimique Indirecte du Xylène, Electrochim. Acta 35 (1990) 273–279.

[26] M. Hamza, S. Ammar, R. Abdelhedi, Electrochemical oxidation of 1,3,5 trimethoxybenzene in aqueous solutions at gold oxide and lead dioxide electrodes, Electrochim. Acta 56 (2011) 3785–3789.

[27] M. Bouaziz, H. Jemai, W. Khabou, S. Sayadi, Oil content, phenolic profiling and antioxidant potential of Tunisian olive drupes, J. Sci. Food Agric. 90 (2010) 1750–1758.

[28] R. Cert, S. Arranz, J. Pérez-Jiménez, A. Cert, F. Saura-Calixto, Comparison between free radical scavenging capacity and oxidative stability of nut oils, Food Chem. 110 (2008) 985–990.

[29] M. Bouaziz, I. Feki, M. Ayadi, H. Jemai, S. Sayadi, Stability of refined olive oil and olive pomace oil added by phenolic compounds from olive leaves, Eur. J. Lipid Sci. Technol. 112 (2010) 894–905.

[30] J. Gruz, O. Novák, M. Strnad, Rapid analysis of phenolic acids in beverages by UPLC–MS/MS, Food Chem. 111 (2008) 789–794.

[31] M. Bouaziz, M. Chamkha, S. Sayadi, Comparative study on phenolic content and antioxidant activity during maturation of the olive cultivar Chemlali from Tunisia, J. Agric. Food Chem. 52 (2004) 5476–5481.

[32] A.P. Kilmartin, H. Zou, L.A. Waterhouse, A cyclic voltammetry method suitable for characterizing antioxidant properties of wine and wine phenolics, J. Agric. Food Chem. 49 (2001) 1957–1965.

[33] D. Galato, K. Ckless, F.M. Susin, C. Giacomelli, M.R. Robeiro-do-Valle, A. Spinelli, Antioxidant capacity of phenolics and related compounds: correlation among electrochemical, visible spectroscopy methods and structure-antioxidant activity, Redox Rep. 6 (2001) 243–250.

[34] O. Firuzi, A. Lacanna, R. Petrucci, G. Marrosu, L. Saso, Evaluation of the antioxidant activity of flavonoids by " ferric reducing antioxidant power" assay and cyclic voltammetry, Biochim. Biophys. Acta 1721 (2005) 174–184.